

# Lithospheric pressure–depth relationship in compressive regions of thickened crust

K. PETRINI<sup>1</sup> AND Yu. PODLADCHIKOV<sup>2</sup>

<sup>1</sup>Institute of Mineralogy and Petrology (katja@erdw.ethz.ch) and <sup>2</sup>Geology Institute, Swiss Federal Institute of Technology, 8092 Zurich, Switzerland

**ABSTRACT** We investigate the pressure distribution with depth in regions undergoing horizontal shortening and experiencing crustal thickening both analytically and numerically. Our results show that, in a convergent tectonic setting, pressure can be considerably higher than lithostatic (the pressure resulting from the weight of the overburden). Increases in pressure with respect to lithostatic conditions result from both the contribution of horizontal stresses and the flexural vertical loads, the latter generated by the deflection of the upper crust and of the mantle because of the presence of topographic relief and a root, respectively. The contribution of horizontal stresses is particularly relevant to the upper crust and uppermost mantle, where rocks are thought to deform brittlely. In these domains, pressure gradients twice lithostatic can be achieved. The contribution of horizontal stresses is less important in the ductile domains as differential stresses are progressively relaxed; nevertheless, the effects are still noteworthy especially close to the brittle–ductile transition. Flexural vertical loads generated by the deflection of the upper crust and lithospheric mantle are relevant for rocks of the weaker lower crust. As a result of the combination of the two mechanisms, the pressure gradient varies vertically through the lithosphere, ranging from negative (inverted) gradients to gradients up to several times the lithostatic gradient. The pressure values range from one to two times the lithostatic values ( $1\rho gz$  to  $2\rho gz$ ).

**Key words:** lithostatic pressure gradient; pressure–depth relationship; pressure gradients two times lithostatic.

## INTRODUCTION

Assessment of the pressure and temperature at which rocks were metamorphosed is of primary importance in the study of a metamorphic terrane because these estimates place important constraints on its tectonic history. While it is widely recognized that the temperature distribution in the lithosphere can vary as a function of the tectonic environment (e.g. England & Thompson, 1984), pressure is thought to increase with depth solely as a function of the overburden weight. Some authors have suggested that the pressure recorded by rocks may differ from lithostatic, in particular to explain the formation of high-pressure rocks such as eclogites and blueschists (Kamb, 1961; Blake *et al.*, 1967; Smith, 1988; Mancktelow, 1993). Some authors suggested that tectonic stresses increase the mean stress (Blake *et al.*, 1967; Brothers, 1970) and have suggested that petrologically derived  $P$ – $T$  paths may not always record depth changes but can also be related to stress changes (e.g. Stüwe & Sandiford, 1994). The increase in mean stress in these high-pressure rocks, however, was assumed to be limited by the maximum differential stresses the lower crust could sustain, the values of which were believed to be as low as 100 MPa (Brace *et al.*, 1970). More recent work has challenged this assumption by recognizing that

perturbations to the mean stress may be greater than the differential stress (Mancktelow, 1995). Mancktelow (1995) demonstrated that specific geometries, related to confined flow, cause significant increases in pressure that are not dependent on the strength of the rocks recording the over-pressure but on their viscosity and on the strength of the ‘container’ causing this increase. Similar results have recently been confirmed by Schmalholz & Podladchikov (1999).

Previous work has focused on localized variations in pressure ascribed ultimately to heterogeneities. The intent of our work is to show that the pressure distribution of the entire lithosphere systematically varies as a function of the tectonic environment. We will show that in a convergent tectonic setting, the pressure is considerably higher than lithostatic through most of the lithosphere. In the stronger regions (upper crust and uppermost mantle), these deviations in pressure are the result of horizontal tectonic stresses. In the weaker lower crust, deviations from lithostatic conditions are caused by flexural loads generated by the undulated topography of the upper crust and the mantle.

In the first section we describe the current lithostatic model and discuss its assumptions. In the following sections we derive analytical pressure–depth relationships for different lithospheric domains. The analytical

predictions are then verified by finite element modelling using a visco-elasto-plastic rheology. The model presented predicts different types of increase in pressure with depth for different rheological behaviours. We suggest that in brittle domains under compression the pressure increase with depth is best approximated by a gradient equal to twice the lithostatic gradient ( $P = 2\rho gz$ ). In the ductile domains, the pressure gradient is extremely variable, and, despite viscous relaxation, significant variations with respect to lithostatic values are produced, ranging from 1 to  $2\rho gz$ .

## ANALYTICAL MODELS FOR PRESSURE-DEPTH GRADIENTS

### Definition of pressure

Pressure,  $P$ , is defined mechanically as the average of the diagonal components of the stress tensor,  $\sigma_{11}$ ,  $\sigma_{22}$  and  $\sigma_{33}$ , where compressional stresses are assumed to be positive:

$$P = \frac{\sigma_{11} + \sigma_{22} + \sigma_{33}}{3} \quad (1)$$

Assuming for simplicity that (a) the maximum compressive principal stress,  $\sigma_1$ , is horizontal and is equal to  $\sigma_{11}$ , (b) the minimum compressive principal stress,  $\sigma_3$ , is vertical and is equal to  $\sigma_{33}$ , and (c) the intermediate component of the principal deviatoric stress tensor is negligible (i.e.  $\sigma_{22} \approx P$ ), the above equation reduces to:

$$P = \frac{\sigma_1 + \sigma_3}{2} \quad (2)$$

Introducing the differential stress  $\Delta\sigma$ , so that  $\Delta\sigma = \sigma_1 - \sigma_3$ , pressure can be expressed as:

$$P = \sigma_3 + \frac{\Delta\sigma}{2} \quad (3)$$

### Lithostatic pressure model

If rocks cannot sustain significant differential stress (i.e.  $\Delta\sigma \approx 0$ ) and the vertical principal stress is identical to the overburden load ( $\sigma_3 = \rho gz$ ), Eq. (3) reduces to the lithostatic relationship:

$$P(z) = \rho gz \quad (4)$$

where  $\rho$  is rock density,  $g$  is the acceleration due to gravity and  $z$  is the depth.

The assumption that rocks cannot sustain significant differential stress could be justified at depths greater than 25 km for quartz rheology or 50 km for olivine rheology (Brace & Kohlstedt, 1980). However, evidence stemming from geophysical observations, for example from earthquake focal mechanisms (Zoback, 1992) or from gravimetric anomalies (Burov *et al.*, 1998), and from laboratory experiments (Brace & Kohlstedt, 1980;

Kohlstedt *et al.*, 1995), has shown that larger differential stresses can be sustained in the upper crust and in the uppermost mantle.

The assumption that the vertical principal stress is identical to the overburden load is generally considered to be valid below the depth of isostatic compensation. Above this depth, however, the isostatic theory implies that deviations are to be expected and have been inferred from gravimetric measurements (Burov & Diament, 1995).

In the following sections we analyse how the lithospheric pressure distribution is influenced by these factors.

### Deviations caused by horizontal stresses

#### Assumptions

In this section we assume that: (a) vertical stress can be approximated with the weight of the overburden rocks ( $\sigma_3 = \rho gz$ ); and, (b) that lithospheric stresses can be approximated by the rock strength as measured in laboratory experiments (Sibson, 1977; Brace & Kohlstedt, 1980). Similar approaches are also presented by Mancktelow (1993) and Weijermars (1993), amongst others. Assumption (b) leads to the distinction of brittle and ductile stress regimes within the lithosphere. The brittle regime is characteristic of the upper crust and the uppermost mantle. In the brittle regime, the relationship between principal stresses can be expressed (see Fig. 1):

$$\frac{\sigma_1 + \sigma_3}{2} \sin(\Phi) = \frac{\sigma_1 - \sigma_3}{2} \quad (5)$$

where  $\Phi$  is the angle of internal friction (Jaeger & Cook, 1979).

The ductile regime is characteristic of the lower crust and of the lower lithospheric mantle, where rock strength depends strongly on temperature, strain rate and grain size.

#### Pressure in the brittle regime

The foregoing assumptions allow us to express the horizontal stresses as a function of depth and the angle

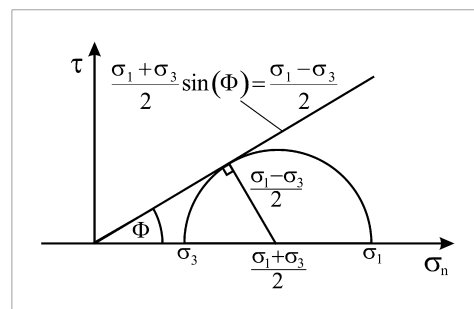


Fig. 1. Mohr circle representation of the relationship between principal stresses along the yield surface.



take hydrostatic restoring forces into account:

$$\Delta P_{lc}(x) = D_{uc} \frac{d^4 W_{uc}}{dx^4} + \rho_c g W_{uc} \quad (12)$$

$$-\Delta P_{lc}(x) = D_{ml} \frac{d^4 W_{ml}}{dx^4} + (\rho_{ml} - \rho_c) g W_{ml} \quad (13)$$

where the subscripts ‘c’, ‘uc’, ‘lc’ and ‘ml’ indicate crust, upper crust, lower crust and mantle lithosphere, respectively,  $x$  is the coordinate in the horizontal direction,  $\rho$  is rock density,  $g$  is the acceleration due to gravity,  $D$  is the flexural rigidity, and  $W_{uc}(x)$  and  $W_{ml}(x)$  are the deflection in the upper crust and mantle relative to a horizontal (relaxed) surface. To clearly distinguish the effects of lithospheric flexure and horizontal stresses, we set the horizontal force to 0.

The geometry of the system (Fig. 2) is constrained so that:

$$\Delta H_{lc}(x) = W_{uc}(x) - W_{ml}(x) \quad (14)$$

where  $\Delta H_{lc}(x)$  is the thickening of the lower crust. We consider the pressure deviation caused by cosine shaped crustal thickening:

$$\Delta H_{lc}(x) = \Delta h_{lc} \cos(2\pi x/\lambda) \quad (15)$$

where  $\Delta h_{lc}$  is the thickening amplitude and  $\lambda$  is the wavelength.

The pressure deviation is obtained as the solution to the system of Eqs (12)–(15):

$$\Delta P_{lc} = \frac{\Delta h_{lc}(-16D_{uc}\pi^4 - \rho_c g \lambda^4)[16D_{ml}\pi^4 + (\rho_m - \rho_c)g\lambda^4]}{(16D_{ml}\pi^4 + g\lambda^4\rho_m + 16D_{uc}\pi^4)\lambda^4} \quad (16)$$

Since any function can be written as the sum of periodic contributions of different wavelengths (Fourier series), the pressure deviations for any arbitrary thickening profile can be reconstructed by linear superposition of its waveforms obtained by applying Eq. (16) to the individual Fourier components (waveforms) of the crustal thickening profile. In the following analysis we focus on a single waveform having  $\Delta h_{lc}$  as the maximum thickening of the mountain belt (for example 30 km for a belt in which an initially 30 km thick crust was doubled in thickness) and  $\lambda$  as alternatively the topography wavelength or the width of the belt. This waveform presumably dominates the topography and therefore it controls the pressure deviation since the amplitudes of the individual waveforms of pressure deviations are proportional to the amplitudes of the topography waveforms.

The relative rigidity of the upper crust and mantle can be represented by the parameter  $a$ :

$$a = \frac{D_{uc}}{D_{uc} + D_{ml}} = \frac{D_{uc}}{D} \quad (17)$$

where  $D$  is approximately the integrated lithospheric

flexural rigidity:

$$D = \frac{T_e^3 E}{12(1-\nu^2)} \quad (18)$$

where  $T_e$  is the lithospheric effective elastic thickness,  $E$  is the Young’s modulus and  $\nu$  is the Poisson ratio.

Thus, Eq. (16) could be reformulated:

$$\Delta P_{lc} = \frac{h_{lc}[16(1-a)D\pi^4 + \rho_c g \lambda^4][16aD\pi^4 + (\rho_m - \rho_c)g\lambda^4]}{[16aD\pi^4 + \rho_m g \lambda^4 + 16(1-a)D\pi^4]\lambda^4} \quad (19)$$

Figure 3 shows pressure deviations from lithostatic in the lower crust ( $\Delta P_{lc}$ ) calculated from the above equation substituting  $E = 1 \times 10^{10}$  Pa,  $\nu = 0.25$ ,  $\rho_c = 2700$  kg m<sup>-3</sup>,  $\rho_m = 3300$  kg m<sup>-3</sup> and  $g = 9.81$  m s<sup>-2</sup>. These results can also be displayed in normalized fashion (Fig. 4) where  $\Delta P_{norm}$  corresponds to the increase in pressure minus the gravitational effect due to topography ( $\Delta P_{lc} - H_{uc}\rho_c g$ ) normalized to the gravitational effect due to thickening ( $H_{lc}\rho_c g$ ). The results (Figs 3 & 4) show that the increase in pressure due to flexural loads depends strongly on the width of the mountain belt ( $\lambda$ ), with wide belts experiencing smaller increases in pressure than narrower belts. By contrast, increased thickening ( $\Delta h_{lc}$ ) and increased effective elastic thickness ( $T_e$ ) result in larger pressure deviations. The results depend also on the relative strength of the bounding plates ( $a$ ). For our plots we have chosen intermediate values, i.e.  $a = 0.5$ , corresponding to the case in which crust and mantle have the same rigidity. The pressure deviations for values of the parameter  $a$  ranging from 0 to 1 can be calculated from Eq. (19), although only intermediate values are likely to have geological relevance because an extremely weak upper crust ( $a \approx 0$ ) or an extremely weak upper mantle ( $a \approx 1$ ) would impede the formation of topographic relief and crustal roots, respectively.

It is worth emphasizing that, for the analysis presented here, the differential stresses were set to 0. This implies that vertical flexural loads allow the lower crust to experience pressure increases with respect to lithostatic without requiring lower crust strength (i.e.  $\Delta \sigma_{lc} = 0$ ).

The presence of vertical flexural load could cause further pressure increases in the lower crust: vertical loads result in increased confining pressure, thus leading to increased rock strength favouring an additional increase through the contribution of horizontal stresses.

## NUMERICAL MODEL

In this section we present a model that was used to determine the pressure in a 2D compressive tectonic setting numerically. This alternative approach, which is independent of the analysis carried out above, enabled us to test the pressure–depth relationship derived analytically (Fig. 5). In comparison to the

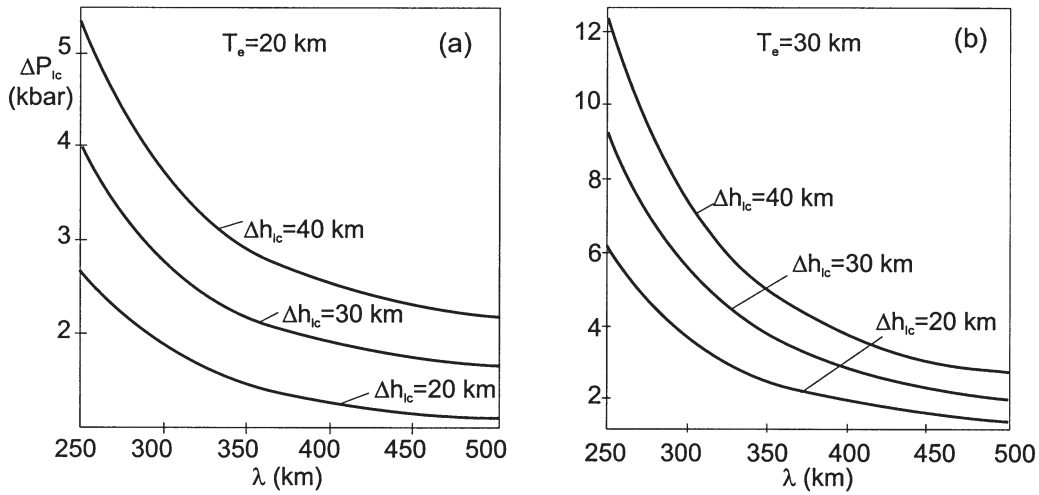


**Fig. 3.** Dependence of magnitude of the deviations from lithostatic pressure on mountain width ( $\lambda$ ), maximum thickening of the lower crust ( $\Delta h_{1c}$ ) and the effective elastic thickness  $T_e$  at a fixed  $a=0.5$  as calculated from Eq. (19) for  $T_e=20$  km (a) and  $T_e=30$  km (b). In both cases, the following material and physical constants were adopted:  $\rho_c=2.7$  kg m $^{-3}$ ,  $\rho_m=3.3$  kg m $^{-3}$ ,  $g=9.81$  m s $^{-2}$ ,  $E=1e11$  Pa and  $\nu=0.25$ .

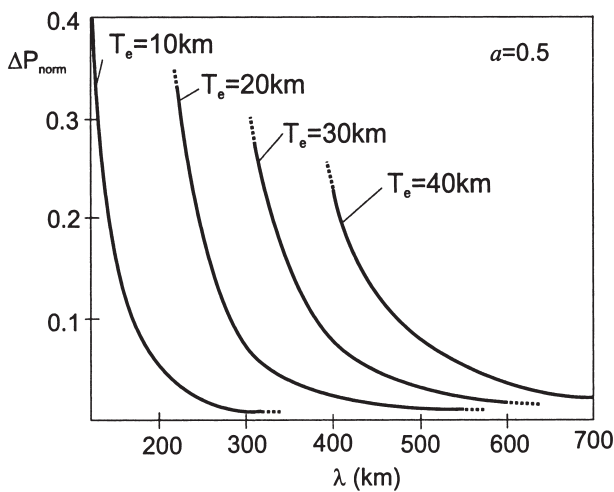


**Fig. 4.** Normalized pressure increase as a function of mountain width at  $a=0.5$ . Different lines represent different effective elastic thickness.

analytical approach, the numerical approach does not distinguish so clearly amongst the contribution of the individual mechanisms; this deficiency, however, is compensated by the possibility of studying the interplay between all the different processes. Furthermore, although a model will always be a simplification compared to nature's complexity, with the present model we were able to incorporate more complexity (e.g. more complex rheologies, the effects of temperature) than was possible in the simple analytical models. The results obtained are in good agreement with the analytical results presented above.

Numerical simulations were carried out using FEMREV, a numerical code developed by Yuri Podladchikov based on an earlier viscous version described in Poliakov and Podladchikov (1992). The

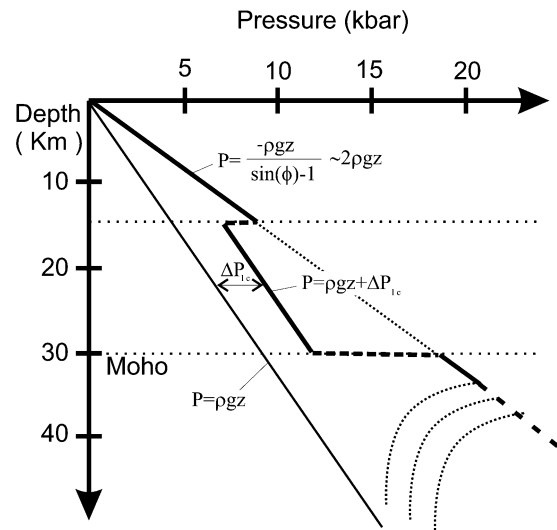


**Fig. 5.** Schematic representation summarizing the results of the analytical model. The pressure model for brittle rheology is applied to the upper crust and the uppermost lithospheric mantle, whereas the model considering flexural loads is applied to the lower crust. In the first case, the pressure gradient is equal to twice the lithostatic gradient. In the second case, the pressure gradient is equal to lithostatic but the pressure values are increased with respect to lithostatic by a fixed deviation ( $\Delta P_{1c}$ ).

2D finite element code incrementally couples plane strain mechanical and thermal calculations. The model (Fig. 6) consists of a box stratified into upper crust (granite rheology), lower crust (diabase rheology) and upper mantle (olivine rheology), deformed by the application of lateral horizontal velocities. The mechanical boundary conditions comprise a lower boundary, fixed in the vertical direction and free to slip in the horizontal direction; sides fixed in the vertical direction and converging with constant velocity; and a free

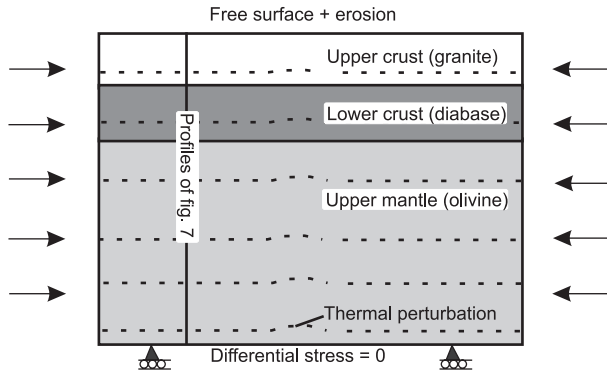


**Fig. 6.** Initial model set-up. The model consists of a box stratified into upper crust (granite rheology), lower crust (diabase) and upper mantle (olivine), deformed by the application of lateral horizontal velocities. Dotted lines represent isotherms.

upper surface subjected to erosion according to hill-slope diffusion. Thermal boundary conditions are constant temperature ( $0^\circ\text{C}$ ) at the surface, fixed temperature at the bottom and no lateral heat flux through the sides. The starting configuration has a relaxed stress state with only gravitational loads and a steady-state temperature distribution with a small thermal perturbation at the bottom to localize deformation.

The stress balance system of equations is:

$$\frac{\partial \sigma_{xx}}{\partial x} + \frac{\partial \sigma_{xz}}{\partial z} = 0 \quad (20)$$

$$\frac{\partial \sigma_{xz}}{\partial x} + \frac{\partial \sigma_{zz}}{\partial z} - \rho(1 - \alpha T)g = 0 \quad (21)$$

where  $\sigma_{ij}$  is the stress tensor and positive sign implies extension,  $T$  is the temperature,  $\alpha$  is the thermal expansion coefficient, and  $z$  is the vertical coordinate directed upwards. The thermal evolution of the model is computed from the heat conduction equation:

$$c\rho \left( \frac{\partial T}{\partial t} + V_x \frac{\partial T}{\partial x} + V_y \frac{\partial T}{\partial y} \right) = k \left( \frac{\partial^2 T}{\partial x^2} + \frac{\partial^2 T}{\partial y^2} \right) + Q \quad (22)$$

where  $t$  is time,  $c$  is the specific heat,  $V_x$  and  $V_y$  are the components of the velocity vector,  $k$  is the heat conductivity and  $Q$  is the volumetric heat production. Adiabatic and strain heating are neglected. The incremental form of Maxwell visco-elastic rheology for deviator components of the stress tensor,  $\tau_{ij}$ , and deviator components of strain rate tensor,  $\dot{\epsilon}_{ij}$ , is:

$$\dot{\epsilon}_{ij} = \frac{1}{2G} \overset{\vee}{\tau}_{ij} + \frac{\tau_{ij}}{2\mu} \quad (23)$$

where  $G$  is the shear modulus,  $\mu$  is the shear viscosity and  $\overset{\vee}{\tau}_{ij}$  is the corotational (Jaumann) objective derivative of the deviatoric stress tensor (e.g. Biot,

1961). The viscosity coefficient,  $\mu$ , is chosen to comply with the uni-axial form of the power law relationship:

$$\dot{\epsilon} = A e^{-E/RT} \Delta \sigma^n \quad (24)$$

where  $R$  is the universal gas constant,  $\dot{\epsilon}$  and  $\Delta \sigma$  are axial strain rate and differential stress, respectively and  $A$ ,  $E$  and  $n$  are material constants (Table 1). Bulk rheology is modelled as elastic. The treatment of yielding follows non-associated Mohr–Coulomb plasticity (Vermeer & de Borst, 1984). At each loading increment, the failure criterion is checked (the frictional angle is set to  $30^\circ$  to comply with Byerlee's law) and instantaneous volume-preserving (the dilation angle is set to zero) plastic deformation is added to maintain the stresses on the failure envelope. For simplicity, fluid pressure is not taken into account.

This set-up, we believe, approximates the mechanical (and thermal) behaviour of a lithosphere subjected to compression. The pressure distribution and its evolution as the lithosphere undergoes horizontal shortening have been studied more closely. Two numerical experiments are presented here. The first experiment simulated compression of a lithosphere with a standard thermal gradient, with the bottom of the lithosphere ( $1250^\circ\text{C}$ ) at 120 km depth. The second experiment simulated compression of a lithosphere with a low thermal gradient, with a 160 km thick lithosphere, representing a continental craton. Parameters are listed in Table 1.

**Table 1.** Model parameters.

Parameter	Value
Length of model	1000 km
Depth of model (base of lithosphere)	Run 1: 120 km Run 2: 160 km
Granitic layer thickness (upper crust)	15 km
Diabase layer thickness (lower crust)	20 km
Olivine layer thickness (upper mantle)	Run 1: 85 km Run 2: 125 km
Temperature at the top	$0^\circ\text{C}$
Temperature at the bottom	$1250^\circ\text{C}$
Convergence rate	$2 \times 10^{-10} \text{ m s}^{-1}$
Bulk modulus	$1 \times 10^{10}$
Shear modulus	$1 \times 10^{10}$
Conductivity	$2.6 \text{ W m}^{-1} \text{ }^\circ\text{C}^{-1}$
Specific heat	$1050 \text{ m}^2 \text{ s}^{-2} \text{ }^\circ\text{C}^{-1}$
<i>Granite properties</i>	
Density of granite ( $T=0^\circ\text{C}$ )	$2700 \text{ kg m}^{-3}$
Power law exponent	3.3
Pre-exponential material parameter ( $A$ )	$3.16 \times 10^{-26} \text{ Pa}^{-n} \text{ s}^{-1}$
Activation energy	$1.9 \times 10^5 \text{ J mol}^{-1}$
Radioactive heat production	$1 \times 10^{-6} \text{ W kg}^{-1}$
<i>Diabase properties</i>	
Density of diabase ( $T=0^\circ\text{C}$ )	$2900 \text{ kg m}^{-3}$
Power law exponent	3
Pre-exponential material parameter ( $A$ )	$3.2 \times 10^{-20} \text{ Pa}^{-n} \text{ s}^{-1}$
Activation energy	$2.76 \times 10^5 \text{ J mol}^{-1}$
Radioactive heat production	$1 \times 10^{-6} \text{ W kg}^{-1}$
<i>Olivine properties</i>	
Density of olivine ( $T=0^\circ\text{C}$ )	$3300 \text{ kg m}^{-3}$
Power law exponent	3
Pre-exponential material parameter ( $A$ )	$7 \times 10^{-14} \text{ Pa}^{-n} \text{ s}^{-1}$
Activation energy	$5.1 \times 10^5 \text{ J mol}^{-1}$

## Results

The pressure distribution deviates significantly from lithostatic conditions (Fig. 7). Pressure increases progressively with strain. At 5% shortening, the deviation of pressure from lithostatic is notable through most of the crust and upper mantle. By 10% shortening, the pressure in the upper crust attains values approximately equal to two times the lithostatic values, closely fitting the analytically established relationship of Eq. (8). Considerable increases with respect to lithostatic pressures are also achieved in the uppermost mantle. The deviation is weaker in the lower crust, where the pressure is not further increased but merely displaced, in accordance with the  $\Delta P$  predicted by the analytical model for flexural loads. Note that at the end of the experiment only 10% shortening is reached. Thus, significant mountain building has not yet taken place, leaving this mechanism of creating over-pressures within the ductile lower crust partially unexploited.

## DISCUSSION

Within the framework of the assumptions made, the results presented document that large deviations from a lithostatic pressure gradient are to be expected throughout the lithosphere. In the case of pressure increase due to the contribution of horizontal stresses, the critical factor is the magnitude of the differential stress in the upper crust and uppermost mantle. To constrain the differential stress level in the analysis presented, we utilized the results from rock mechanics laboratory experiments, which are quantitatively well documented (Brace & Kohlstedt, 1980; Kohlstedt *et al.*, 1995). These data are consistent with recent, indepen-

dent estimates of lithospheric strength based on gravimetric analyses (Burov *et al.*, 1998). Based on these data, our results constitute an extreme situation that leads to the maximum deviation. The computed pressure gradients would be reduced by stresses below the rock strength in the brittle regime or by effective rock strengths less than those assumed.

Increased vertical stresses lead to increases in pressure in the lower crust independent of its strength and therefore this mechanism does not suffer from the above limitations. It constitutes an example of a tectonic over-pressure that is not limited by the strength of the rocks recording the increase in pressure but by the rheology of the entire system (Mancktelow, 1995), in this case the lithosphere. The deviations in pressure resulting from this mechanism make it difficult to relate pressures to depth. The analytical model presented can be used to estimate the pressure deviations resulting from flexural loads. However, this application is limited by several uncertainties. First, the calculated pressure deviations are strongly sensitive to the parameters (see Figs 3 & 4). Second, although it is possible to obtain estimates of the parameters (e.g. lower crustal thickening, width of the mountain belt and effective elastic thickness) for present-day mountain belts, it is more difficult to estimate the appropriate values for exhumed collision zones.

### Thermodynamic pressure

An important consideration in the relation of pressure to depth is the nature of the thermodynamic potential interpreted as the pressure recorded by geobarometers. Indeed, at high differential stresses, it is legitimate to question the validity of classical thermodynamics,

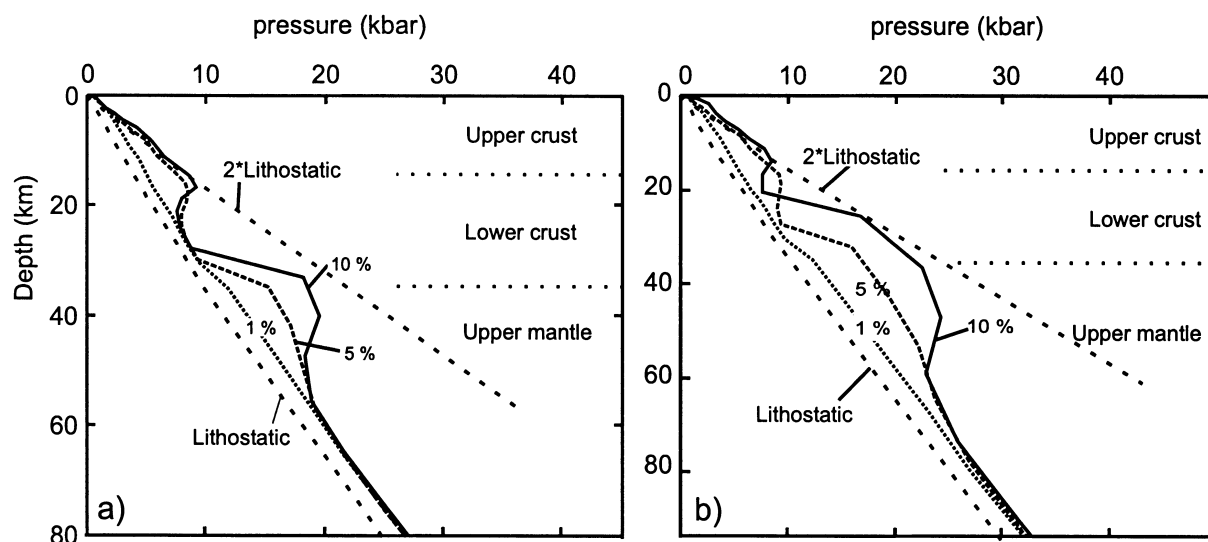


Fig. 7. Pressure distribution with depth at different percentage shortening for (a) 120 km thick lithosphere, and (b) 160 km thick lithosphere. The line indicated 'lithostatic' corresponds to a lithostatic pressure gradient ( $P = l\rho gz$ ); the other lines correspond to the pressure resulting from the model at different stages of shortening.

which was originally developed for fluids, for determining the equilibrium conditions in non-hydrostatically stressed solid systems. It is uncertain whether, for non-hydrostatic conditions, it is appropriate to equate pressure with the average of the normal stresses, or whether it would be more appropriate to use the maximum principal stress, or the stress component normal to the boundary of the reactant phase. Several authors have devoted considerable effort to deriving thermodynamic theories for non-hydrostatically stressed solids (Kamb, 1961; Kumazawa, 1963; Paterson, 1973; Truskinovskij & Kuskov, 1982; Dahlen, 1992; Bartholomeusz, 1995). Laboratory experiments supporting these theories show that phase transitions can be affected by non-hydrostatic conditions (Green, 1986; Reynard *et al.*, 1996). However, in most cases, the magnitude of non-hydrostatic corrections to pressure estimates is smaller than the uncertainty of geobarometers. For this reason, in our discussion we assume that the results of mineral geobarometry indicate the pressure of formation of the assemblage (or mineral) in question.

#### *The effects of high stresses on temperature*

Differential stresses are likely to affect not only the pressure but also the temperature, through a phenomenon that has recently regained attention and is alternatively named shear heating (e.g. Stüwe, 1998; Harrison *et al.*, 1999; amongst many), strain heating (e.g. Wan *et al.*, 1986; Perchuk *et al.*, 1992) or viscous dissipation (e.g. Shchipansky & Podladchikov, 1994; Kincaid & Silver, 1996). It is worth emphasizing that the phenomenon is not linked exclusively to friction along fault zones but can play an important role in any system undergoing irreversible deformation (references above). Assuming no heat exchange with the surroundings, a simple estimate of the stress contribution to temperature for loaded rocks can be expressed as (Chang & Cozzarelli, 1977):

$$c\rho \frac{\partial T}{\partial t} = \tau_{ij} \dot{\epsilon}_{ij} \quad (25)$$

and assuming constant deviatoric stress the magnitude of the temperature increase can be assessed by time integration:

$$\Delta T = \int \frac{\partial T}{\partial t} dt = \int \frac{\tau_{ij} \dot{\epsilon}_{ij}}{c\rho} dt = \frac{\tau_{ij}}{c\rho} \epsilon_{ij} \quad (26)$$

where  $\epsilon_{ij}$  is the total strain achieved during deformation.

As an example, a strain of 100% and differential stresses of 300 MPa, assuming a heat capacity of  $c = 1000 \text{ J kg}^{-1} \text{ K}^{-1}$  and a density of  $\rho = 3000 \text{ kg m}^{-3}$ , would cause a temperature increase of  $c. 100^\circ\text{C}$ .

Such an increase in temperature would reduce lithospheric strength and thus partially reduce the magnitude of stress effects on pressure and on

temperature. Further work will be required to study the interplay between these different mechanisms in more detail.

#### THERMAL AND GEOLOGICAL IMPLICATIONS

Unfortunately, any relation for the determination of depth from pressure, be it one of the models presented above or the conventional lithostatic model, is very difficult to verify with geological observation because there is no way of determining depth independently of pressure except for very shallow levels. Measurements of *in situ* stress magnitude, performed to a maximum of 7 km depth, indicate that the horizontal stresses rarely define a lithostatic gradient but usually define lines that corresponds to the Mohr–Coulomb failure criterion envelopes (McGarr & Gay, 1978; Zoback & Healy, 1984; Brudy *et al.*, 1997)

A chance to test the validity of the model presented to greater crustal depths is provided by preserved pressure gradients in metamorphic terranes. These are generally considerably steeper than lithostatic pressure gradients, but this could be misleading as the inference of field pressure gradients is complicated by at least two major problems. First,  $P$ – $T$  arrays do not necessarily correspond to  $P$ – $T$  gradients (e.g. Thompson & England, 1984), and second, the steep slope of pressure gradients could be solely the result of tectonic thinning of the metamorphic pile. Nevertheless, we present an example from the well-studied Franz Josef-Fox Glacier area in the New Zealand Southern Alps (Adams, 1981; Allis, 1986; Grapes & Watanabe, 1992; Kamp & Tippett, 1993), where very careful observations enable these difficulties to be overcome. In this area, Grapes & Watanabe (1992) were able to reconstruct an average pressure gradient of  $1 \text{ kbar km}^{-1}$  over a structural thickness of 4 km. Petrological observations in these schists are in conflict with significant shortening of the sequence after peak metamorphism, because an apparently complete prograde garnet–oligoclase zone mineral sequence is not retrogressed (Grapes & Watanabe, 1992).

Steep and/or inverted pressure gradients and anomalous high pressures, similar to those predicted by our model, are also typical of metamorphic ‘soles’ beneath ophiolites. Two main problems pertain to geological observations in these terranes. First, the pressure recorded at the top of the sequences (directly below the ophiolites) is ‘too large’ compared to the thickness of the ophiolite. For example, the pressure estimate for the formation of garnet amphibolites beneath the Semail ophiolite is approximately 1.1 GPa (Gnos, 1998). Calculations using the lithostatic relationship and an average density of  $2800 \text{ kg m}^{-3}$  yield a thickness of nearly 40 km. The Semail ophiolite, although characterized by a remarkable thickness, does not exceed 20 km (Gnos, 1998). Second, within these ophiolitic ‘soles’, pressure usually decreases

down-depth (inverted pressure gradient) and the gradient often is extremely steep, with metamorphism ranging from near eclogitic facies down to greenschist facies in the space of a few hundred metres (e.g. Spray & Williams, 1980; McCaig, 1983; Jamieson, 1986; Gnos, 1998). As these terranes are often located close to the crustal brittle-ductile transition (10–20 km depth), we argue that the observed features might correspond to the negative and extremely steep pressure gradient produced by our model at depths corresponding to this transition.

Problematic pressures and pressure distributions also characterize high-pressure terranes. Occurrences of high- and very-high-pressure phases such as coesite and diamond in metamorphic terranes are common (e.g. Chopin, 1984; Coleman & Wang, 1995; Dobretsov *et al.*, 1995; Hacker *et al.*, 1997). The estimated pressures at which such phases have formed can reach 3 GPa (e.g. Chopin *et al.*, 1991; Hacker *et al.*, 1997). Assuming a lithostatic pressure gradient ( $P = \rho gz$ ), these occurrences would imply that large portions of crustal rocks must be buried to depths exceeding 100 km. These depths are believed to be impossible to reach by burial resulting from crustal thickening, and therefore subduction is usually advocated to reach the required conditions. However, considering the depths inferred, even subduction is not devoid of difficulties for crustal rocks. The viability of this mechanism remains to be proven for the buoyant crustal material (e.g. Molnar & Gray, 1979). The mechanisms presented here, which can lead to the formation of high-pressure parageneses at shallower depth (e.g. 2 GPa and 600 °C are reached at 40 km depth), suggest an alternative explanation that does not require exceptional burial depths. The reduction of the burial depth by the contribution of a tectonically generated pressure component would on one hand facilitate the formation of high-pressure mineral assemblages by subduction and on the other hand rehabilitate crustal thickening as an alternative formation setting. It is worth emphasizing that the mechanism we suggest for the establishment of supra-lithostatic pressures in the lower crust, i.e. the contribution of flexural vertical loads, does not require high deviatoric stresses and is therefore compatible with microstructural observation suggesting little deformation in these high-pressure rocks.

Even greater problems than those posed by the formation of very-high-pressure rocks are presented by their exhumation. This can be testified by the number of recent publications concerned with the variety of exhumation models that have been proposed (e.g. Cloos, 1982; Platt, 1986; Chopin *et al.*, 1991; Chemenda *et al.*, 1995). Platt (1993) has compiled a list of features commonly observed in high-pressure terranes against which exhumation models should be tested. This list includes constraints in time and in geological setting. With some exceptions, exhumation occurs during convergence (e.g. Michard *et al.*, 1993) and in the early stages of the orogenic cycle (Winkler & Bernoulli,

1986; Michard *et al.*, 1994; Boundy *et al.*, 1996) thus preceding the exhumation of terranes exhibiting Barrovian-type metamorphism. Moreover, Platt (1993) has outlined the presence in many high-pressure terranes of significant pressure gaps and pressure inversions, i.e. decreasing pressure with increasing structural depth (Blake *et al.*, 1967; Jayko *et al.*, 1987; Hacker *et al.*, 1997).

The pressure model proposed here leads to the fulfilment of the constraints listed above. Indeed compression is necessary to achieve and maintain high pressures. Furthermore the mechanisms presented are thought to be the most efficient in the initial stages of continental convergence, because during the initial thickening phases the spacing between the isotherms is increased, which leads to an overall lithospheric strengthening. This strengthening would favour a significant tectonic contribution to pressure. In the following stages, however, the geotherm would increase towards the pre-thickening geotherm and significant heating would result from the advection of deeply buried material. Weakening would be the mechanical consequence of heating and the tectonically originated pressure contribution would be decreased, changing the type of metamorphism from high- $P$  to Barrovian. Moreover, the numerical experiments presented predict the existence of depth regions with inverted pressure gradients. These regions are located immediately below the brittle-ductile transition, approximately in depth ranges between 15 and 20 km. The model results also indicate the presence of extremely high pressure gradients (up to 2 kbar  $\text{km}^{-1}$ ), which in the case of sporadic sampling or of small displacement along late faults could result in the observed pressure gaps.

High pressure gradients have implications also in the derivation of geothermal gradients when these are derived by equating pressure to depth. Figure 8 shows how the geothermal gradient would rotate with respect

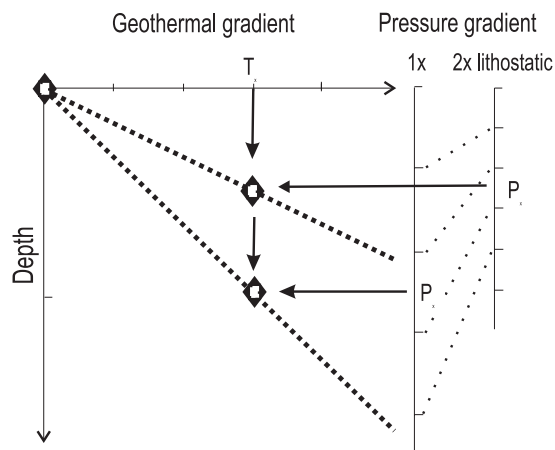


**Fig. 8.** Projection of the geothermal gradient on two different pressure–depth axes. The gradient rotates with respect to the depth axis if the pressure axis is stretched as a function of the pressure model adopted.

to the depth axis as a function of the pressure model adopted. Thus, the same increase in temperature with depth could result in two different 'apparent' temperature gradients depending on whether a lithostatic pressure gradient or a higher pressure gradient is adopted. In the first case, the temperature gradient will appear smaller than in the second (Fig. 8).

## CONCLUSIONS

We have presented two mechanisms capable of increasing pressure with respect to lithostatic conditions in compressive tectonic settings. The first mechanism is an increase ascribable to the contribution of horizontal tectonic stresses. This mechanism is relevant for the upper crust and uppermost mantle, where the rocks are deformed brittlely. In these domains the pressure gradient may be twice the lithostatic gradient ( $P = 2\rho gz$ ). In the ductile lower crust, the effects of the horizontal stresses diminish progressively. However, close to the crustal brittle-ductile transition and at the interface with the mantle, considerable variations persist also in the lower crust. Furthermore, in regions of thickened crust, the ductile regions are likely to experience the greatest variations in pressure because of vertical loads generated by the deflections resulting from the presence of topographic relief and its roots.

## ACKNOWLEDGEMENTS

We thank A. B. Thompson, J. Connolly, G. Simpson, N. Mancktelow, J. Ridley and J.-P. Burg for stimulating discussion and for significantly improving the scientific content as well as the English of the several different versions of this script. We are also grateful to K. Stüwe, E. Burov and J. Selverstone for the thorough and very useful reviews. We are also thankful to D. Yuan for encouragement and to C. Chopin for profitable discussion.

## REFERENCES

- Adams, C. J., 1981. Uplift rates and thermal structure in the Alpine Fault Zone and Alpine Schists, Southern Alps, New Zealand. In: *Thrust and Nappe Tectonics* (eds McClay, K. R. & Price, N. J.). Geological Society Special Publication, London, **9**, 211–221.
- Allis, R. G., 1986. Mode of crustal shortening adjacent to the Alpine Fault, New Zealand. *Tectonics*, **5**, 15–32.
- van Balen, R. T. & Podladchikov, Y., 1998. The effect of inplane force variations on a faulted elastic thin-plate, implications for rifted sedimentary basins. *Geophysical Research Letters*, **25**, 3903–3906.
- van Balen, R. T., Podladchikov, Y. & Cloetingh, S., 1998. A new multilayered model for intraplate stress-induced differential subsidence of faulted lithosphere, applied to rifted basins. *Tectonics*, **17**, 938–954.
- Bartholomeusz, B. J., 1995. The chemical potential at the surface of a non-hydrostatically stressed defect-free solid. *Philosophical Magazine A*, **71**, 489–495.
- Biot, M. A., 1961. Theory of folding of stratified viscoelastic media and its implications in tectonics and orogenesis. *Geological Society of America Bulletin*, **72**, 1595–1620.
- Blake, M. C., Irwin, W. P. & Coleman, R. G., 1967. Upside-down metamorphic zonation, blueschist facies, along a regional thrust in California and Oregon. *U.S. Geological Survey Professional Papers*, **575/C**, 307–328.
- Boundy, T. M., Essene, E. J., Hall, C. M., Austrheim, N. & Halliday, A. N., 1996. Rapid exhumation of lower crust during continent–continent collision and late extension: evidence from Ar–Ar incremental heating of hornblendes and muscovites, Caledonian orogen, western Norway. *Geological Society of America Bulletin*, **108**, 1425–1437.
- Brace, W. F. & Kohlstedt, D. L., 1980. Limits on lithospheric stress imposed by laboratory experiments. *Journal of Geophysical Research*, **85B**, 6248–6252.
- Brace, W. F., Ernst, W. G. & Kallberg, R. W., 1970. An experimental study of tectonic overpressure in Franciscan rocks. *Geological Society of America Bulletin*, **81**, 1325–1338.
- Brothers, R. N., 1970. Lawsonite–albite schists from northernmost New Caledonia. *Contributions to Mineralogy and Petrology*, **25**, 185–208.
- Brudy, M., Zoback, M. D., Fuchs, K., Rummel, F. & Baumgartner, J., 1997. Estimation of the complete stress tensor to 8 km depth in the KTB scientific drill holes: implications for crustal strength. *Journal of Geophysical Research – Solid Earth*, **102B**, 18453–18475.
- Burov, E. B. & Diament, M., 1995. The effective elastic thickness ( $T_e$ ) of continental lithosphere: what does it really mean? *Journal of Geophysical Research*, **100B**, 3905–3927.
- Burov, E., Jaupart, C. & Marechal, J. C., 1998. Large-scale crustal heterogeneities and lithospheric strength in cratons. *Earth and Planetary Science Letters*, **164**, 205–219.
- Chang, W. P. & Cozzarelli, F. A., 1977. On the thermodynamics of nonlinear single integral representations for thermoviscoelastic materials with application to one-dimensional wave propagation. *Acta Mechanica*, **25**, 187–206.
- Chemenda, A. I., Mattauer, M., Malavieille, J. & Bokun, A. N., 1995. A mechanism for syn-collisional deep rock exhumation and associated normal faulting: results from physical modelling. *Earth and Planetary Science Letters*, **132**, 225–232.
- Chopin, C., 1984. Coesite and pure pyrope in high-grade pelitic blueschists of the western Alps: a first record and some consequences. *Contributions to Mineralogy and Petrology*, **86**, 107–118.
- Chopin, C., Henry, C. & Michard, A., 1991. Geology and petrology of the coesite-bearing terrain, Dora Maira massif, Western Alps. *European Journal of Mineralogy*, **3**, 263–291.
- Cloos, M., 1982. Flow melanges: numerical modelling and geological constraints on the origin in the Franciscan subduction complex. *Bulletin of the Geological Society of America*, **93**, 330–345.
- Coleman, R. G. & Wang, X., 1995. *Ultra-high Pressure Metamorphism*. Cambridge University Press, Cambridge.
- Dahlen, F. A., 1992. Metamorphism of nonhydrostatically stressed rocks. *American Journal of Science*, **292**, 184–198.
- Dobretsov, N. L., Sobolev, N. V., Shatsky, V. S., Coleman, R. G. & Ernst, W. G., 1995. Geotectonic evolution of diamondiferous paragneisses, Kokchetav Complex, northern Kazakhstan: the geologic enigma of ultrahigh-pressure crustal rocks within a Paleozoic foldbelt. *Island Arc*, **4**, 267–279.
- England, P. C. & Thompson, A. B., 1984. Pressure–temperature–time paths of regional metamorphism I. Heat transfer during evolution of regions of thickened continental crust. *Journal of Petrology*, **25**, 894–928.
- Gnos, E., 1998. Peak metamorphic conditions of garnet amphibolites beneath the Semail ophiolite: implications for an inverted pressure gradient. *International Geology Review*, **40**, 281–304.
- Grapes, R. & Watanabe, T., 1992. Metamorphism and uplift of Alpine Schist in the Franz Josef-Fox glacier area of the Southern Alps, New Zealand. *Journal of Metamorphic Geology*, **10**, 171–180.
- Green, H. W. II, 1986. Phase transformation under stress and Volume transfer creep. In: *Mineral and Rock Deformation: Laboratory Studies; the Paterson Volume* (eds Hobbs, B. E., Heard, H. C.), pp. 201–211. American Geophysical Union, Washington, DC, USA.

- Hacker, B. R., Wang, X., Eide, E. A. & Ratschbacher, L., 1997. Qinling-Dabie ultrahigh-pressure collisional orogen. In: *The Tectonics of Asia* (eds Yin, A. & Harrison, T. M.) pp. 345–370.
- Harrison, T. M., Grove, M., McKeegan, K. D., Coath, C. D., Lovera, O. M. & Le Fort, P., 1999. Origin and episodic emplacement of the Manaslu intrusive complex, central Himalaya. *Journal of Petrology*, **40**, 3–19.
- Hynes, A., Arkani-Hamed, J. & Greiling, R., 1996. Subduction of continental margins and the uplift of high-pressure metamorphic rocks. *Earth and Planetary Science Letters*, **140**, 13–25.
- Jaeger, J. C. & Cook, N. G. W., 1979. *Fundamentals of Rock Mechanics*. Chapman & Hall, London.
- Jamieson, R., 1986. *P-T* paths from high temperature shear zones beneath ophiolites. *Journal of Metamorphic Geology*, **4**, 3–22.
- Jayko, A. S., Blake, M. C. & Harms, T., 1987. Attenuation of the Coast Range ophiolite by extensional faulting, and nature of the Coast Range 'thrust', California. *Tectonics*, **6**, 475–488.
- Kamb, W. B., 1961. The thermodynamic theory of nonhydrostatically stressed solids. *Journal of Geophysical Research*, **66**, 259–271.
- Kamp, P. J. J. & Tippett, J. M., 1993. Dynamics of Pacific Plate crust in the South Island (New Zealand) zone of oblique continent-continent convergence. *Journal of Geophysical Research—Solid Earth*, **98B**, 16105–16118.
- Kincaid, C. & Silver, P., 1996. The role of viscous dissipation in the orogenic process. *Earth and Planetary Science Letters*, **142**, 271–288.
- Kohlstedt, D. L., Evans, B. & Mackwell, S. J., 1995. Strength of the lithosphere: constraints imposed by laboratory experiments. *Journal of Geophysical Research*, **100B**, 17587–17602.
- Kumazawa, M., 1963. A fundamental thermodynamic theory on nonhydrostatic field and on the stability of mineral orientation and phase equilibrium. *Journal of Earth Sciences Nagoya University*, **11**, 145–217.
- Kuszniir, N. J. & Matthews, D. H., 1988. Deep seismic reflections and the deformational mechanics of the continental lithosphere. *Journal of Petrology*, **10**, 63–87.
- McCaig, A., 1983. *P-T* conditions during emplacement of the Bay of Islands ophiolite complex. *Earth and Planetary Science Letters*, **65**, 459–473.
- McGarr, A. & Gay, N. C., 1978. State of stress in the Earth's crust. *Annual Review Earth Planetary Science*, **6**, 405–436.
- Mancktelow, N. S., 1993. Tectonic overpressure in competent mafic layers and the development of isolated eclogites. *Journal of Metamorphic Geology*, **11**, 801–812.
- Mancktelow, N. S., 1995. Nonlithostatic pressure during sediment subduction and the development and exhumation of high pressure metamorphic rocks. *Journal of Geophysical Research*, **100B**, 571–583.
- Michard, A., Chopin, C. & Henry, C., 1993. Compression versus extension in the exhumation of the Dora-Maira coesite-bearing unit, Western Alps, Italy. *Tectonophysics*, **221**, 173–193.
- Michard, A., Goffé, B., Saddiqi, O., Oberhänsli, R. & Wendt, A. S., 1994. Late Cretaceous exhumation of the Oman blueschists and eclogites: a two-stage extensional mechanism. *Terra Nova*, **6**, 404–413.
- Molnar, P. & Gray, D., 1979. Subduction of continental lithosphere: some constraints and uncertainties. *Geology*, **22**, 999–1002.
- Paterson, M. S., 1973. Nonhydrostatic thermodynamics and its geologic applications. *Reviews of Geophysics and Space Physics*, **11**, 355–389.
- Poliakov, A. & Podladchikov, Yu., 1992. Hydrodynamic modelling of some metamorphic processes. *Journal of Metamorphic Geology*, **10**, 311–319.
- Platt, J. P., 1986. Dynamics of orogenic wedges and the uplift of high-pressure metamorphic rocks. *Geological Society of America Bulletin*, **97**, 1037–1053.
- Platt, J. P., 1993. Exhumation of high-pressure rocks: a review of concepts and processes. *Terra Nova*, **5**, 119–133.
- Podladchikov, Y., 1996. Diapirism and topography. *Geophysical Journal International*, **109**, 553–564.
- Ranalli, G., 1987. *Rheology of the Earth*. Allen and Unwin, Boston.
- Reynard, B., Fiquet, G., Itie, J. P. & Rubie, D. C., 1996. High pressure X-ray diffraction study and equation of state of MgSiO<sub>3</sub> ilmenite. *American Mineralogist*, **81**, 45–50.
- Schmalholz, S. & Podladchikov, Y., 1999. Buckling versus folding: importance of viscoelasticity. *Geophysical Research Letters*, **26**, 2641–2644.
- Shchipansky, A. A. & Podladchikov, Y., 1994. 'Heard batholiths' as indicators of thick early Archean oceanic crust. *Transactions (Doklady) USSR Academy of Sciences, Earth Science Section*, **321a**, 63–67.
- Sibson, R. H., 1977. Fault rocks and fault mechanism. *Journal of the Geological Society of London*, **133**, 191–213.
- Smith, D. C., 1988. A review of the peculiar mineralogy of the 'Norwegian coesite-eclogite province', with crystal-chemical, petrological, geochemical and geodynamical notes and an extensive bibliography. In: *Eclogites and Eclogite-Facies Rocks* (ed. Smith, D. C.), pp. 1–206, Elsevier, Amsterdam.
- Spray, J. C. & Williams, G. D., 1980. The sub-ophiolite metamorphic rocks beneath the Bellantrae igneous complex, South West Scotland. *Journal of the Geological Society of London*, **137**, 359–386.
- Stüwe, K., 1998. Heat sources of Cretaceous metamorphism in the Eastern Alps – a discussion. *Tectonophysics*, **287**, 251–269.
- Stüwe, K. & Sandiford, M., 1994. Contribution of deviatoric stress to metamorphic *P-T* paths: an example appropriate to low-*P*, high-*T* metamorphism. *Journal of Metamorphic Geology*, **12**, 445–454.
- Thompson, A. B. & England, P. C., 1984. Pressure-temperature-time paths of regional metamorphism II. Their inference and interpretation using mineral assemblages in metamorphic rocks. *Journal of Petrology*, **25**, 929–955.
- Truskinovskij, L. M. & Kuskov, O. L., 1982. Chemical equilibria in a nonhydrostatic system. *Geokhimiya*, **12**, 1798–1812.
- Tsenn, M. C. & Carter, N. L., 1987. Upper limits of power law creep of rocks. *Tectonophysics*, **136**, 1–26.
- Turcotte, D. L. & Schubert, G., 1982. *Geodynamics*. John Wiley & Sons, New York.
- Vermeer, P. A. & de Borst, R., 1984. Non-associated plasticity for soils, concrete and rock. *Heron*, **29**, 1–64.
- Wan, K. T., Cozzarelli, F. A. & Hodge, D., 1986. Creep strain-heating due to folding. *Physics of the Earth and Planetary Interiors*, **43**, 56–66.
- Weijermars, R., 1993. Estimation of paleostresses orientation within deformation zones between two mobile plates. *Geological Society of America Bulletin*, **105**, 1491–1510.
- Winkler, W. & Bernoulli, D., 1986. Detrital high-pressure/low temperature minerals in a late Turonian flysch sequence of the eastern Alps (western Austria): Implications for early Alpine tectonics. *Geology*, **14**, 598–601.
- Zoback, M. L., 1992. Stress field constraints on intraplate seismicity in eastern North America. *Journal of Geophysical Research*, **97**, 11761–11782.
- Zoback, M. D. & Healy, J. H., 1984. Friction, faulting and in situ stress. *Annales Geophysicae*, **2/6**, 689–698.

Received 25 May 1999; revision accepted 7 September 1999.